Refereed Proceedings

The 13th International Conference on Fluidization - New Paradigm in Fluidization Engineering

Engineering Conferences International *Year* 2010

TIME-AVERAGED MODELLING OF CFBS – ANALYSIS OF THE TERMS IN THE MOMENTUM EQUATIONS

Sirpa Kallio* Maiju Seppälä†

Veikko Taivassalo‡

*VTT, Finland

†VTT, Finland, maiju.seppala@vtt.fi

‡VTT, Finland

TIME-AVERAGED MODELLING OF CFBS – ANALYSIS OF THE TERMS IN THE MOMENTUM EQUATIONS

Sirpa Kallio, Maiju Seppälä, Veikko Taivassalo
VTT, P.O.Box 1000, FI-02044 VTT, Finland

ABSTRACT

The features of the terms in the time-averaged momentum equation for the solid phase are examined for three CFB units ranging from a laboratory-scale unit to a small CFB boiler. The CFD simulations were based on the Eulerian granular model of the Fluent software. The time-averaged terms calculated during the time-dependent simulations are analysed and conclusions on their relative importance are drawn. An analysis of the terms in the vertical solids momentum equation in the central region of a CFB is presented.

INTRODUCTION

Today dense multiphase flows are usually modelled as time dependent. As transient multiphase simulations commonly require a small time step and a fine mesh, CFD simulations of fluidized beds typically demand significant computing resources. Especially in case of large industrial CFB units, steady-state multiphase modelling can thus be an attractive alternative. The multiphase closure models developed for time-dependent modelling are not as such applicable in steady-state simulations. Additional terms resulting from the time-averaging process need to be closed. The closure models are crucial since in steady-state simulations, a larger portion of momentum transfer is expressed by closure models than in transient simulations. Therefore, steady-state simulations rely more on the closure relations and especially on the models for inter-phase momentum transfer and for the Reynolds stress terms.

Several attempts to develop closure models for coarse-mesh and steady-state simulations have been presented in the literature. Agrawal et al. (1), Andrews et al. (2), Igci et al. (3), and Zhang and VanderHeyden (4) studied the average drag and stress terms. In Zhang and VanderHeyden (5), an added-mass force closure was suggested for the correlation between fluctuations of the pressure gradient of the continuous phase and fluctuations of solids volume fraction. De Wilde (6) analysed the same term from simulations and accounted also for the drag force in the derivation of new closure models that were applied in De Wilde et al. (7) for steady-state simulation of a riser. Zheng et al. (8) presented a two-scale Reynolds stress turbulence model for gas-particle flows. The closure models mentioned above are mainly based on transient simulations in a fairly small scale.

TIME-AVERAGED CFD MODELLING OF CFB PROCESSES

Time-averaged equations used in steady-state simulations are developed by averaging the corresponding transient equations over time. A number of new terms arising due to correlations between fluctuations in velocities, voidage, and local stresses have to be modelled to close the equation system. Closure relations can be derived by analyzing measurements and/or results from transient simulations. In this work, time-dependent simulations were conducted and validated by measurements.

The momentum equation used in the transient simulations can be written for phase *q* (gas phase denoted by *g* and solid phase by *s*) as follows:

$$\frac{\partial \alpha_q \rho_q u_{q,i}}{\partial t} + \frac{\partial \alpha_q \rho_q u_{q,k} u_{q,i}}{\partial x_k} = -\alpha_q \frac{\partial p}{\partial x_i} + \frac{\partial \alpha_q (\tau_{q,ik} + \tau^M_{q,ik})}{\partial x_k} - \frac{\partial p_s}{\partial x_i}\delta_{qs} + \alpha_q \rho_q g_i + (-1)^{(\delta_{qs}+1)} K_{gs}\left(u_{g,i} - u_{s,i}\right) \quad (1)$$

where *t* is time, *x* a spatial coordinate, *α* volume fraction, *ρ* density, *u* velocity, *p* gas phase pressure, p_s solids pressure, *g* gravitational acceleration, *K* drag coefficient, δ_{qs} Kronecker delta, τ laminar stress, and τ^M local scale turbulent stress. A time-averaged momentum equation is obtained by averaging Equation (1) over time. A time average, also called Reynolds average, of a variable ϕ is defined as

$$\bar{\phi} = \frac{1}{\Delta t}\int_t^{t+\Delta t} \phi dt \quad (2)$$

The instantaneous values can now be written as $\phi = \bar{\phi} + \phi'$. The time average is used as such for the volume fraction α_q and pressure *p*. A Favre average or a phase-weighted average is defined as follows

$$\langle \phi \rangle = \overline{\alpha_q \phi} \;/\; \overline{\alpha_q} \quad (3)$$

Favre averaging is applied on velocities and we denote the average velocity by $U_{q,i} \equiv \langle u_{q,i} \rangle$. For the instantaneous velocity we have then $u_{q,i} = U_{q,i} + u_{q,i}''$. We obtain now the time-averaged momentum equation for a phase *q*

$$\frac{\partial \bar{\alpha}_q \rho_q U_{q,k} U_{q,i}}{\partial x_k} = \bar{\alpha}_q \rho_q g_i - \bar{\alpha}_q \frac{\partial \bar{p}}{\partial x_i} - \overline{\alpha_q' \frac{\partial p'}{\partial x_i}} + \frac{\partial \overline{\alpha_q \tau_{q,ik}}}{\partial x_k}$$

$$+ \frac{\partial \overline{\alpha_q \tau^M_{q,ik}}}{\partial x_k} + (-1)^{(\delta_{qs}+1)} \overline{K_{gs}\left(u_{gi} - u_{si}\right)} - \frac{\partial \bar{p}_s}{\partial x_i}\delta_{qs} - \frac{\partial \rho_q \overline{\alpha_q u_{q,k}'' u_{q,i}''}}{\partial x_k} \quad (4)$$

The terms on the right hand side are the gravitation term, pressure term, pressure fluctuation term, laminar stress, turbulent stress, drag force, solid pressure term, and the Reynolds stress term. The gravitation and pressure terms can be calculated from the basic average flow properties but the rest need to be modelled.

On basis of an analysis of the time-averaged results of a simulation of a CFB pilot, Kallio et al. (9) found that the three main terms to be modelled in the time-averaged momentum equation are the drag, Reynolds stress, and pressure fluctuation terms. In addition to these three terms, the averages of the laminar and turbulent stress terms and the average solids pressure require modelling. Kallio et al. (9) showed, however, that these terms are relatively small in the major part of a CFB. In this paper we concentrate on the central upper part of the CFB riser, where we focus on the drag force, the pressure fluctuation term, the solids pressure term and the Reynolds stress term in the axial solids momentum equation.

OVERVIEW OF THE SIMULATIONS

A large number of time-dependent simulations for analysis of time-averaged properties were carried out. For this paper eight 2D simulations, listed in Table 1, were selected. Three different geometries were included: the 2D laboratory scale CFB unit at Åbo Akademi University (ÅA), the Chalmers boiler, and the cold pilot CFB unit of Foster Wheeler in Karhula, Finland.

Table 1. Case details. (*W*: riser width, *D*: depth, *H*: height, U_0: superficial gas velocity, d_p: particle diameter, Re_p Reynolds number, v_t: terminal velocity, Δt_{total}: simulated time period).

Case	Geometry	*W* x *D* x *H* m x m x m	U_o m/s	d_p mm	ρ_p kg/m^3	Re_p #)	v_t m/s	Δt_{total} s
1	ÅA	0.4 x 0.015 x 3	3.15	0.385	2480	75	2.9	1393
2	ÅA	0.4 x 0.015 x 3	3.25	0.44	2480	99	3.3	123
3	ÅA	0.4 x 0.015 x 3	3.75	0.44	2480	99	3.3	124
4	ÅA	0.4 x 0.015 x 3	2.75	0.256	2480	45	2.2	129
5	ÅA	0.4 x 0.015 x 3	2.75	0.256	2480	3.0	1.5	105
6	Chalmers	1.62 x 1.42 x 13.5 *)	5.8	0.250	2600	2.7	1.5	656
7	Karhula	1.0 x 0.25 x 7.3	3.0	0.23	1800	20	1.3	333
8	Karhula	1.0 x 0.25 x 7.3	5.0	0.23	1800	20	1.3	250

#) case 5: ρ_g=0.31 kg/m^3, μ_g=4.45·10^{-5} kg/ms, all other cases: ρ_g=1.225 kg/m^3, viscosity μ_g=1.79·10^{-5} kg/ms
*) below 2.2 m the cross-section is 1.42 m x 1.42 m

In the cases of Chalmers and Karhula CFBs, modifications were done to the geometry to allow 2D simulations. In addition, the geometries were selected such that the superficial gas flow rate at each height corresponded to the one in the 3D experiment. Comparisons to measurements in the ÅA geometry were presented in (10) and in the Karhula geometry in (9). The conditions for the Chalmers simulation (Case 6) were chosen from Zhang et al. (11). In the chosen case there is no secondary air flow and the uniform bed temperature is 850 ºC. The actual Sauter mean diameter in the experiments was 0.33 mm. To better describe the average particle size in the upper part of the riser, the particle size used was reduced to 0.25 mm.

Time-dependent CFD simulations were conducted with the Fluent software (12) using the same kinetic theory based hydrodynamic models as in (9). In Cases 1-3 a uniform mesh with mesh spacings of 6.25 mm was used. In Cases 4 and 5 the mesh was otherwise the same but in the bottom region up to 0.7 m height the spacings were halved. In Case 6 mesh spacings were 20 mm except for the wall regions were the mesh was refined in the lateral direction. In Cases 7 and 8 the mesh spacings varied in the vertical direction from 43 mm at the bottom to 49 mm at the top and in the lateral direction from 14 mm at the walls to 41 mm in the centre.

In Cases 1-5 the gas-solids drag was calculated from the Ergun (13) equation in the dense suspension regions up to 80% voidage while in the more dilute regions the equation of Wen & Yu (14) was applied. In Cases 7 and 8 the drag correction function used in (9) was applied on the drag to counteract the effects of the significant small-scale clustering that is not correctly produced by the CFD simulation in a coarse mesh. In Case 6 the correction function was modified to take into account the differences in phase properties and mesh spacings. The correction functions, with which the single particle drag law is multiplied, are shown in Fig. 1.

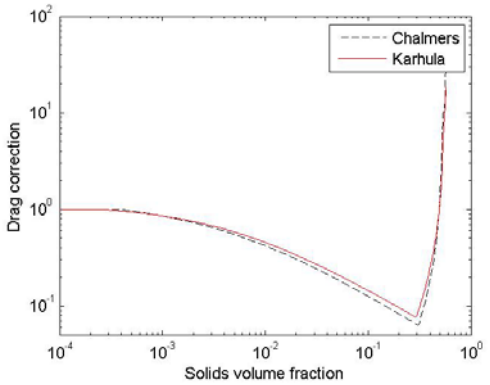

Fig. 1. Correction functions applied to the single particle drag law.

RESULTS

The time-averaged terms in Eq. (4) were calculated for all the eight cases. Plots of the average volume fractions obtained in three simulations and the 2D geometries are shown in Fig. 2. In industrial CFBs the major part of the flow domain is dilute and far from walls and thus also our analysis concentrates on the terms in similar flow conditions. Close to the walls, at riser bottom and at riser exit the flow patterns and consequently also the behaviour of the balance equation terms are more complicated. The studied regions are depicted in Fig. 2.

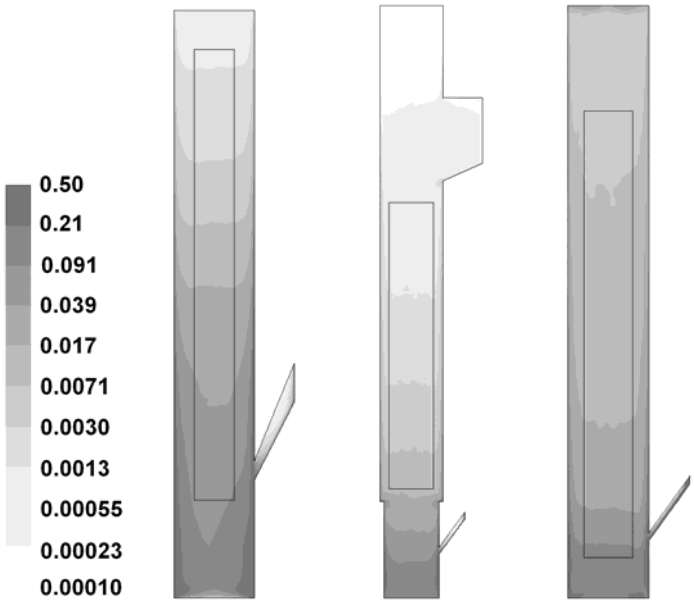

Fig. 2. Logarithmic solids volume fraction contours and geometries of the simulated cases: a) Åbo Akademi pilot scale riser b) Chalmers boiler c) Karhula CFB pilot. The areas considered in the analysis are marked by the rectangular boxes.

We concentrate on the terms in the vertical momentum equation for the solid phase and start the analysis from the gas-particle drag term. In dilute conditions, the local instantaneous drag force is calculated from the equation of Wen & Yu (14). Thus a good measure of clustering effects on the average drag would be the deviation from

a drag force that is calculated from the equation of Wen & Yu (14). For comparison we thus calculate in every point of the flow domain this theoretical drag force $K^*_{gs}(U_{g,y}-U_{s,y})$, where K^*_{gs} is calculated from the averaged quantities:

$$K^*_{gs} = \frac{3\overline{\alpha_s}\rho_g}{4d_s\overline{\alpha_g}^{1.65}} C_D\left|U_g-U_s\right|,\ C_D=\frac{24\left(1+0.15(\mathrm{Re}_p\,\overline{\alpha_g})^{0.687}\right)}{\mathrm{Re}_p\,\overline{\alpha_g}},\ \mathrm{Re}_p=\frac{\rho_g d_s\left|U_g-U_s\right|}{\mu_g} \quad (5)$$

and divide it with the time-averaged vertical drag force $\overline{K_{gs}\left(u_{gi}-u_{si}\right)}$.

The resulting drag ratio in each mesh point inside the region marked in Fig. 2a is depicted in Fig. 3a for Case 1. In the entire region the ratio stays above one indicating that clustering has reduced the average drag force acting on the particles. We note an almost linear relationship between the drag ratio and the logarithm of the solids volume fraction. Thus a linear function is fitted to the data. Fig. 3b compares the corresponding linear functions obtained from all the eight simulations. No big difference is seen between Cases 1, 2 and 3, in which the material properties of gas and solids are similar. In Case 4, where the particles were smaller, the obtained drag ratio is higher indicating stronger clustering. In the hot conditions of Case 5, with the same particle size as in Case 4, the drag ratio is even higher. In Case 6, i.e. in the simulation of the Chalmers boiler, the drag ratio is significantly higher than in the other cases. In this case the drag was already strongly reduced during the calculation to account for the coarse mesh, which can have affected the results. Similarly in Cases 7 and 8 a drag correction function was used during the transient simulations, which makes the results somewhat unreliable.

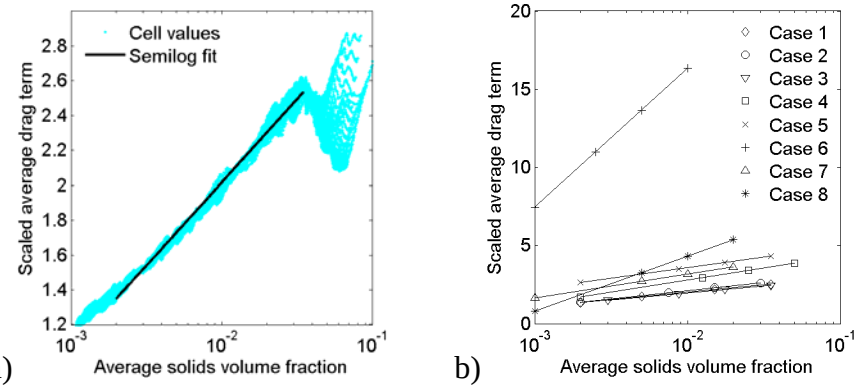

a) b)

Fig. 3. a) Time-averaged vertical drag force in the studied region in Case 1 divided by the theoretical drag calculated from Eq. (5) and a linear fit to the data. b) The corresponding fitted lines in all the eight cases.

The values obtained for the other terms in Eq. (4) were scaled by dividing by the time-averaged vertical drag force to facilitate the comparisons between different terms. Contours of the average vertical drag force per solids mass in Case 1 are shown in Fig. 4a. The ratio between the vertical Reynolds stress term and the average vertical drag force is shown in Fig. 4b and the ratio between the solids pressure term and the average vertical drag force in Fig. 4c. Fig. 4a shows clearly the reduction in the drag force in the intermediate solids concentration range characterized by extensive clustering. According to Fig. 4b, the Reynolds stress term is of the same order of magnitude with the drag term in the major part of the

flow domain. No simple relationship between the Reynolds stress term and other flow properties was found. Thus a more rigorous model is required.

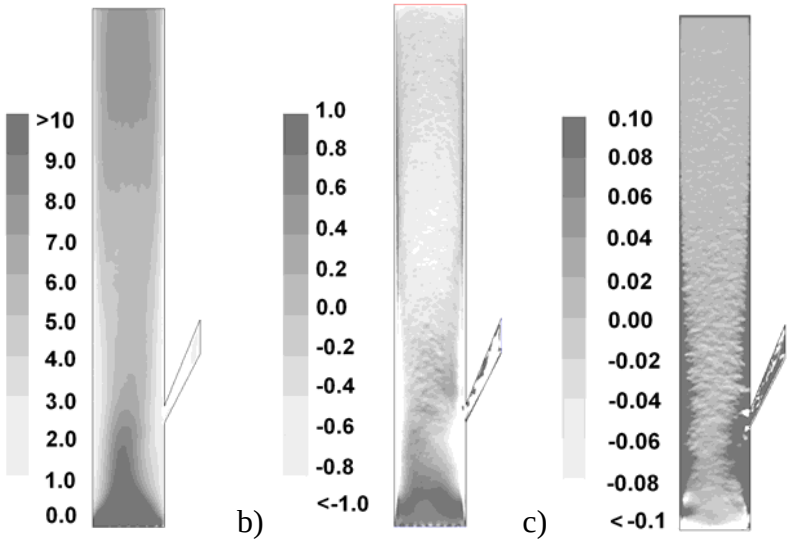

a) b) c)

Fig. 4. Case 1: a) Contours of the average vertical drag force per solids mass. b) The ratio of the vertical Reynolds stress term to the average vertical drag. c) The ratio of the average solids pressure term to the average vertical drag force.

In Fig. 5a, the pressure fluctuation term divided by the average drag is shown as a function of solids volume fraction. Again a linear relationship is obtained and linear functions (Fig. 5b) are fitted to the data in the eight cases. On basis of the results from Cases 1-5, the ratio between the pressure fluctuation term and the drag force decreases with voidage and is unaffected by the particle size and the Reynolds number. The results from Cases 6-8 differ, which can be due to the coarser mesh that affects the way fluctuations are produced in the simulation. In the literature, the pressure fluctuation term has been modelled through an added mass term (e.g. De Wilde (6), Zhang & VanderHeyden (5)). The pressure fluctuation term produced by the model of De Wilde (6) was compared with the values obtained from the simulation of Case 1. The pressure fluctuation term produced by the model was of a completely different character than what we observe in our simulations.

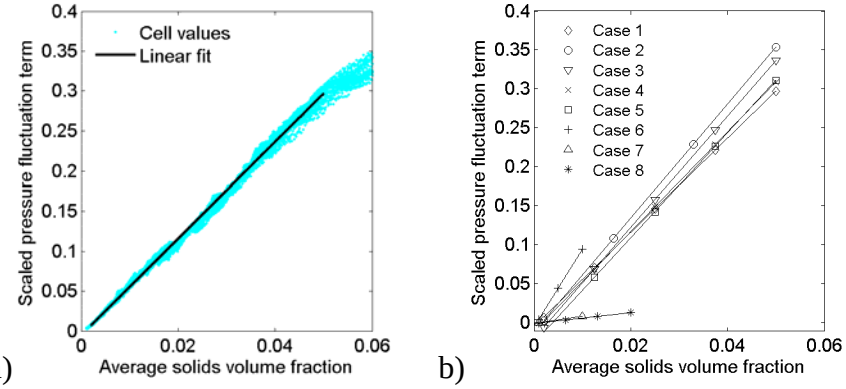

a) b)

Fig. 5. a) Time-averaged vertical pressure fluctuation term divided by the average vertical drag force in the studied region in Case 1 as a function of solids volume fraction and a linear fit to the data. b) The corresponding fitted lines in all the eight cases.

The average solids pressure term shown in Fig. 6c is small compared to the average drag and pressure fluctuation terms in the solids vertical momentum equation. However, in the lateral equation it is a significant term. A linear correlation of the average solids pressure with the square of the average volume fraction was observed (Fig. 6a.) and thus linear functions could be fitted to the data in all the eight cases, see Fig. 6b. A clear increase in the average solids pressure is seen as a function of solids volume fraction. In addition, the average solids pressure increases as a function of the particle Reynolds number. In the coarse mesh simulations in Cases 6-8, solids pressure is lower. In a coarse mesh, the simulation fails to produce very high local solids volume fractions that would be required for high values of local solids pressure. Thus coarse mesh simulations are not suitable for estimation of solids pressure.

A similar analysis of the terms could be done for the lateral time-averaged momentum equation. The relative importance of the different terms, e.g. of the solids pressure term, differs from the situation in the vertical equation. The lateral drag force, however, is very small which complicates the comparisons of different terms.

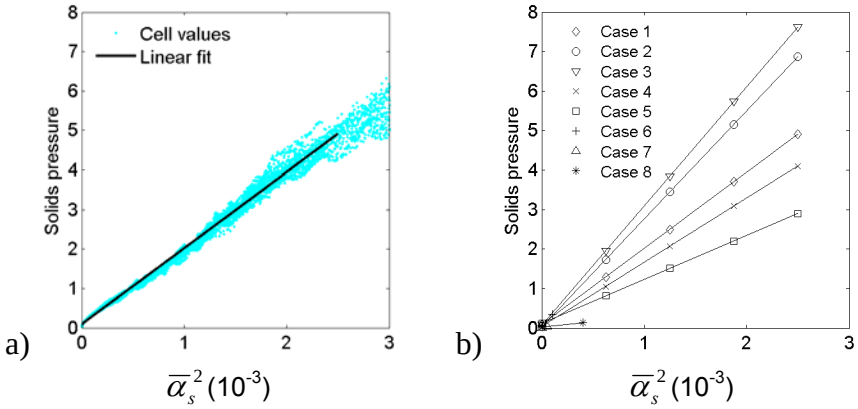

Fig. 6. a) Time-averaged solids pressure as function of the square of the average solids volume fraction in the studied region in Case 1 and a linear fit to the data. b) The corresponding fitted lines in all the eight cases.

CONCLUSIONS

An analysis of the terms in the time-averaged vertical momentum equation for the solid phase was conducted for eight cases and for three CFB units ranging from a laboratory-scale unit to a small CFB boiler. The analysis was based on time-averaging the results from time-dependent simulations. An analysis of the terms in the time-averaged vertical solids momentum equation in the central region of a CFB was presented. There the largest terms are the drag term and the Reynolds stress term. A clear reduction in the average drag force per solids mass was observed in the intermediate solids concentration range where significant clustering takes place. This reduction in the average drag force is largest for small particles and it also increases with the gas temperature. The average pressure fluctuation term was found to increase with the average drag force and the ratio of the average pressure fluctuation term to the average drag force could be described by a simple linear function of the average solids volume fraction. For average solids pressure in the

analyzed cases, a relationship with the average solids volume fraction and the particle Reynolds number was found.

ACKNOWLEDGEMENTS

The authors gratefully acknowledge the financial support of Tekes, VTT Technical Research Centre of Finland, Fortum Oyj, Foster Wheeler Energia Oy, Neste Oil Oyj and Metso Power Oy.

REFERENCES

(1) Agrawal, K., Loezos, P.N., Syamlal, M., Sundaresan, S., The role of meso-scale structures in rapid gas-solid flows, J.Fluid Mech. 445, pp. 151-185, 2001.
(2) Andrews, A.T., Loezos, P.N., Sundaresan, S., Coarse-grid simulation of gas-particle flows in vertical risers, Ind. Eng. Chem. Res. 44, pp. 6022-6037, 2005.
(3) Igci, Y., Sundaresan, S., Pannala, S., O'brien, T., Breault, R.W., Coarse-graining of two-fluid models for fluidized gas-particle suspensions, 5th Int. Conf. on CFD in the Process Industries, CSIRO, Melbourne, Australia, 2006.
(4) Zhang, D.Z., VanderHeyden, W.B., High-resolution three-dimensional numerical simulation of a circulating fluidized bed, Powder Tech. 116, pp. 133-141, 2001.
(5) Zhang, D.Z., VanderHeyden, W.B., The effects of mesoscale structures on the macroscopic momentum equations for two-phase flows, Int. J. of Multiphase Flow 28, pp. 805-822, 2002.
(6) De Wilde, J., The generalized added mass revised, Physics of Fluids 19, 058103, 2007.
(7) De Wilde, J., Heynderickx, G.J., Martin, G.B., Filtered gas-solid momentum transfer models and their application to 3D steady-state riser simulations, Chem. Eng. Sci. 62, pp. 5451-5457, 2007.
(8) Zheng, Zh.X., Zhou, L.X., A two-scale second-order moment particle turbulence model and simulation of dense gas–particle flows in a riser, Powder Tech. 162, pp. 27-32, 2006.
(9) Kallio, S., Taivassalo, V., Hyppänen, T., Towards time-averaged CFD modelling of circulating fluidized beds, 9th Int Conf. on Circulating Fluidized Beds, Hamburg, May 12-16, 2008.
(10) Kallio, S., Guldén, M., Hermanson, A.: Experimental study and CFD simulation of a 2D circulating fluidized bed, The 20th Int. Conf. on Fluidized bed combustion. Xi'an, China, 2009.
(11) Zhang, W., Johnsson, F., Leckner, B., Fluid-dynamic boundary layers in CFB boilers, Chem. Eng. Sci. 50, pp. 201-210, 1995.
(12) Fluent Inc., Fluent Users' guide – Release 6.0, 2001.
(13) Ergun, S., Fluid flow through packed columns, Chemical Engineering Progress, 48, pp. 89-94, 1952.
(14) Wen, C.Y., Yu, Y.H., Mechanics of fluidization, Chemical Engineering Progress Symposium Series, Vol. 66, No. 62, pp. 100-111, 1966.